

# Sub-23 nm particulate emissions from a highly boosted GDI engine

Felix Leach<sup>1</sup>, Andrew Lewis<sup>2</sup>, Sam Akehurst<sup>2</sup>, James Turner<sup>2</sup>, David Richardson<sup>3</sup>

1. Department of Engineering Science, University of Oxford, UK

2. University of Bath, UK

3. Jaguar Land Rover Ltd. UK

SAE Technical Paper – Author's Accepted Manuscript

## Abstract

The European Particle Measurement Program (PMP) defines the current standard for measurement of Particle Number (PN) emissions from vehicles in Europe. This specifies a 50% count efficiency ( $D_{50}$ ) at 23 nm and a 90% count efficiency ( $D_{90}$ ) at 41 nm. Particulate emissions from Gasoline Direct Injection (GDI) engines have been widely studied, but usually only in the context of PMP or similar sampling procedures. There is increasing interest in the smallest particles – i.e. smaller than 23 nm – which can be emitted from vehicles. The literature suggest that by moving  $D_{50}$  to 10 nm, PN emissions from GDI engines might increase by between 35 and 50% but there remains a lot of uncertainty. In this work, an existing data set from the Ultraboost engine – a highly boosted engine running at up to 32 bar BMEP – has been evaluated using two filtering methodologies, one with a 50% count efficiency ( $D_{50}$ ) at 10 nm and a 90% count efficiency ( $D_{90}$ ) at 23 nm (Filter 1) and the other with a  $D_{50}$  at 10 nm and a  $D_{90}$  at 15 nm (Filter 2) and the results have been compared to PMP equivalent filtering. The effect of engine parameters relevant to highly boosted engines such as exhaust back pressure, EGR, spark and injection timing is analysed, as well as the effect of fuel composition. The results show that an increase in PN emissions of 36% with Filter 1 and 45% with Filter 2 is on average observed with the two different count efficiencies with the baseline fuel.

## Introduction

Particle number (PN) emissions from light duty vehicles have been regulated in Europe since 2011 (diesel) and 2014 (petrol) – currently at a level of  $6 \times 10^{11}$  #/km. The sampling methodology for PN emissions is governed by the Particle Measurement Program (PMP) [1]. Typically particulates emitted from light duty vehicles fall in a size range of 5-1000 nm [2]. PN emissions from Gasoline Direct Injection (GDI) engines have been a topic of research interest for some time [3] particularly because the reduced time for mixture formation compared to Port Fuel Injected (PFI) engines can lead to higher particulate emissions [4]. However, due to their lower CO<sub>2</sub> emissions than previous engine technologies, GDI engines are widely used in the market. Particulate emissions from GDI engines are typically bilognormal in distribution, with two clear modes – the nucleation mode from 10-40 nm (typically consisting of volatile and semi-volatile particles) and the accumulation mode from 40-200 nm (typically consisting of solid particles with adsorbed material).

Currently the PMP protocol requires the use of a volatile particle remover that extracts most of the nucleation mode particulates. PMP compliant systems count particles using a Condensation Particle Counter (CPC) and compliant CPCs are required to have a 50% count efficiency at  $d_p = 23$  nm, and > 90% count efficiency at  $d_p = 41$  nm [1]. PMP adopted these count efficiencies to ensure that only solid particles were being measured, because of the high sensitivity of volatile particles to sampling conditions (i.e. they can move in and out of gas phase quickly and easily) and hence poor repeatability of the measurements of such particles [5].

However the existence of solid particles below 23 nm being emitted from GDI engines has long been known. Gidney *et al.* [6] found that certain metal anti-knock additives in gasoline gave rise to substantial solid particle emissions around 10 nm in diameter. Giechaskiel *et al.* [7] in a comprehensive literature survey reported that in general GDI vehicles emitted 30-40% PN below 23 nm, which is currently unmeasured by PMP compliant procedures. Jang *et al.* [8] found that under certain driving conditions up to 80% of the particles emitted from a GDI engine were below 23 nm. Solid particle emissions below 23 nm are also reported from diesel and PFI engines [7, 9]. The standard for measuring PN emissions from aircraft engines already specifies a  $D_{50}$  cut size of 10 nm [10].

Recently research is being undertaken to investigate PN emissions from GDI vehicles below 23 nm. Giechaskiel *et al.* [11] conducted a study of eight different vehicles, including two GDI vehicles over NEDC and WLTP cycles to measure the fraction of particles below 23 nm. They reported that for GDI engine vehicles the fraction below 23 nm was between 35 and 50%. Significant efforts are underway to improve the accuracy of particulate measurement below 23 nm such as Down To Ten [12], SUREAL-23 [13], and PEMs4Nano [14]. The EU Joint Research Centre (JRC) is investigating the feasibility of moving the PMP  $D_{50}$  cut size to 10 nm and actively monitoring PN emissions below 23 nm [15].

Increasing GDI engine boost has been shown to reduce particulate emissions, however it has also been shown to reduce the mean particle diameter and increase levels of PN below 23 nm which has been attributed to reductions in flame size as boost is increased [16, 17]. Karjalainen *et al.* [18] tested a boosted 1.8 L GDI vehicle and reported that a major share of the particle emissions were below 23 nm. Bogarra *et al.* [19] also reported that a substantial fraction of particles downstream of a three-way catalyst (TWC) were below 23 nm – and there was strong evidence to show that the TWC was removing volatile particles when fully warm. There is

therefore substantial evidence in the literature to show that boosted GDI engines emit a significant number of particles which are not counted by the current standard.

Braisher *et al.* [20] showed that the PMP protocol can be replicated using a Differential Mobility Spectrometer (DMS) to measure PN emissions – this allows the fast, transient nature of DMSs such as the Cambustion DMS500 to be exploited. Braisher *et al.* demonstrated that evaluating the DMS500 accumulation mode bilognormal fit, the PN emissions results follow PMP compliant results closely (because the PMP effectively discounts nucleation mode particles) – equivalent results can be found elsewhere in the literature [21]. Braisher *et al.* also showed that PMP equivalent results could be obtained by applying a Wiebe filter (Equation 1) digitally to the outputs from a DMS.

$$f = 1 - \exp \left[ -3.54 \left( \frac{d_p - 14}{40} \right)^{1.09} \right], \quad (d_p \geq 14) \quad (1)$$

$$f = 0, \quad (d_p < 14)$$

Subsequent work by some of this study's authors [17] showed that the digital filtering approach was essential when considering PN emissions from highly boosted GDI engines due to the small diameters of accumulation mode particles observed.

In this work particulate emissions from a highly boosted engine that were previously measured and reported [17, 22, 23] have been reassessed with a new lower  $D_{50}$  cut size of 10 nm in order to evaluate the effect of this lower cut size relative to the established methodologies. The results reported in this previous work showed that the accumulation mode particles were very small; with accumulation mode diameters of less than 40 nm observed on market fuels and with some fuels accumulation mode diameters of less than 30 nm were observed. As a result, this is a particularly interesting dataset to investigate the impact of particulate emissions with a diameter less than 23 nm.

## Experimental methodology

The aim of this work was to investigate what effect moving the  $D_{50}$  cut size for particle number measurement from 23 nm to 10 nm would have on the total PN emitted using a previously published dataset [17, 22, 23].

Detailed discussion of the experimental methodology for these tests is included in the reports of the results of those tests [17, 22, 23], however a number of key parameters of interest for highly boosted engines were varied such as: engine load, fuel injection pressure, lambda ( $\lambda$ ), inlet air temperature, exhaust gas recirculation (EGR), exhaust back pressure (EBP), fuel injection timing, and ignition timing.

All of the PN emissions measured in the dataset were taken with a Cambustion DMS500. The operating principle of the DMS500 has been described by Reavell *et al.* [24]. The DMS500 uses electrical mobility of particles to give particle size distributions of particles between 5-1000 nm. For the datasets evaluated in this work, the DMS500 remote cyclone and sampling lines were all maintained at 150°C, and the dilution ratio (single stage dilution only) was set to 10 : 1.

The particle size distributions from the previously reported results have been re-filtered with two new Wiebe functions. These functions were chosen to provide two options for evaluation of particles sub-23nm. Both

have a  $D_{50}$  cut at 10 nm (Equation 2), however the first has a  $D_{90}$  cut at 23 nm chosen to effectively shift the current standard to the smaller size -  $D_{50}$  from 23nm to 10 nm and  $D_{90}$  from 41 nm to 23 nm. The second has a  $D_{90}$  cut at 15 nm (Equation 3) which has been chosen to mimic a candidate CPC for measurement at 10 nm from the PEMS4Nano program [25] and to better match the shape of the initial filter (Equation 1). The initial filter Equation 1 is also presented below as a comparison.

$$f_{original} = 1 - \exp \left[ -3.54 \left( \frac{d_p - 14}{40} \right)^{1.09} \right], \quad (d_p \geq 14) \quad (1)$$

$$f = 0, \quad (d_p < 14)$$

$$f_1 = 1 - \exp \left[ -3.80 \left( \frac{d_p - 4}{30.7} \right)^{1.04} \right], \quad (d_p \geq 4) \quad (2)$$

$$f = 0, \quad (d_p < 4)$$

$$f_2 = 1 - \exp \left[ -4.00 \left( \frac{d_p - 4}{14.7} \right)^{1.96} \right], \quad (d_p \geq 4) \quad (3)$$

$$f = 0, \quad (d_p < 4)$$

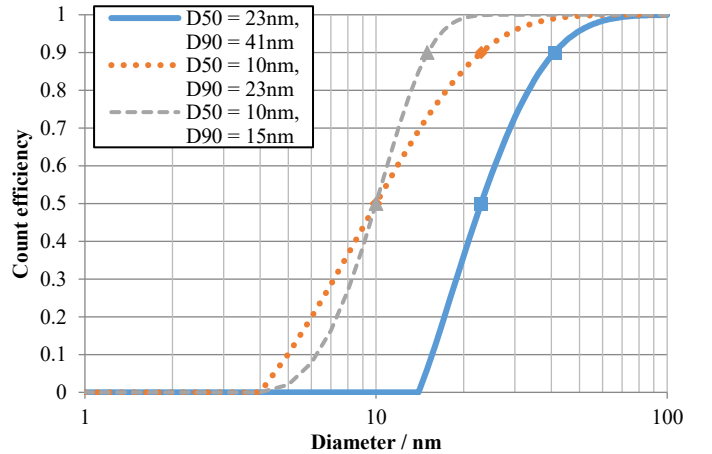


Figure 1: Comparison Wiebe functions showing  $D_{50}$  at 23 nm and a  $D_{90}$  at 41 nm (solid line),  $D_{50}$  at 10 nm and a  $D_{90}$  at 23 nm (dotted line), and  $D_{50}$  at 10 nm and a  $D_{90}$  at 15 nm (dashed line)

These digital filters are multiplied by the raw particle spectrum which is output from the DMS500 to give a total particle count. In this work the filter with the  $D_{90}$  cut at 23 nm (Equation 2) is known as Filter 1 and the filter with the  $D_{90}$  cut at 15 nm (Equation 3) is known as Filter 2. It is acknowledged that when using a DMS, there is no way of knowing whether a particle is solid or liquid phase, however, given the previous success of using Wiebe filters to mimic the PMP protocol [20] it is of interest to apply a similar method to investigate sub-23 nm particulate emissions.

## Engine

The tests were all conducted on the UB100 Ultraboost engine. The UB100 engine is a ‘proof-of-concept’ prototype engine and an introduction to this engine is given in Turner *et al.* [26]. Several prototype features were present on this engine, notably that no turbocharger and supercharger were fitted; rather their functions are provided using an external charging system known as the Combustion Air Handling Unit (CAHU) in conjunction with an Exhaust Back Pressure (EBP) valve. The engine was not fitted with any aftertreatment – of particular note in this instance is that there was no TWC, which has been shown to remove volatile particles [19, 20] and no particle filter. The specifications of the engine are shown in Table 1.

Table 1: Specifications of the test engine

Engine	UB100
Type	In-line 4 cylinder
Bore × Stroke	83 × 92 mm
Displacement	1991 cm <sup>3</sup>
Valves per cylinder	2 intake, 2 exhaust
Compression ratio	9:1
Maximum fuel pressure	200 bar
Aspiration	External boost

## Test conditions

Test conditions were selected to mimic typical GDI engine operation (within a homologation drive cycle envelope, in this case a point of high residence over a New European Drive Cycle), as well as to test the operating envelope of the system. The test conditions used in this work are explained fully in [17], however for convenience a summary is shown in Table 2.

Table 2: Engine test conditions

Test Condition	1	2	3	4
Engine speed (rpm)	1250	2000	3000	4000
Load	3.77 bar BMEP	Boosted WOT, KLSA*	Boosted WOT, KLSA*	Boosted WOT, KLSA*
Number of spark timings tested	8	10	10	3
Parameter varied	EGR (0-10%)	Inlet air temperature (20-40°C) and fuel injection timing (3 timings)	Exhaust Back Pressure (Super-turbo charged transition)	$\lambda$ (1.0-0.875)

\*Wide Open Throttle, Knock Limited Spark Advance – i.e. full load

## Test fuels

The fuels tested in this work were not selected with PN emissions measurement particularly in mind (and it is known that fuel composition has a significant effect on PN emissions [27, 28]); however they represent

a large spread of the fuels likely to be used in highly boosted engines. Full details of these fuels and their composition is given in [22, 23], and a brief overview is included here and in Table 3. The fuels are split into three categories: Market Representative Fuels, Specially Blended Test Fuels, and Oxygenate Fuels. Within the Market Representative Fuels, the Base Fuel is an EN228 [29] compliant gasoline (with 5% v/v ethanol) representative of UK market fuel, Fuel H is a minimum RON EN228 fuel (with 5% v/v ethanol), and Fuel I is similar to a market “premium” gasoline (winter grade). Within the Specially Blended Test Fuels, Fuels A-D represent a deconvolved RON-MON matrix and were used to test the sensitivity of the engine to those parameters, Fuels E and F have high and low laminar flame speeds respectively, and Fuel G is a fuel with artificially boosted RON. Within the Oxygenate Fuels E20 (gasoline with 20% v/v ethanol), E85 (gasoline with 85% v/v ethanol), and a GEM fuel (a blend of gasoline ethanol and methanol designed for iso-stoichiometry with E85) were tested.

Table 3: Test fuel specifications

Fuel	RON (-)	MON (-)	DVPE (kPa)	FBP (°C)
A	103.3	95	26.1	177
B	101.4	88.8	68.0	176
C	92.8	90.7	30.5	193
D	88.6	87.3	32.9	190
E	95.1	82.2	28.7	138
F	104.2	92.6	23.3	139
G	111.6	101.2	57.4	192
H	95.1	85.0	53.1	189
I	98.7	86.5	97.4	173
Base	97.0	85.3	75.0	188
E20	99.6	85.7	57.8	184
E85	107.4	89.5	44.4	78
GEM	106.0	88.1	84.4	74

## Results

All of the results are presented as a “PN increase factor”, which is the factor by which the number of particles has increased when filtered with the new filter compared to the original number of particles observed. A “PN increase factor” of 1 means that there is no increase in the number of particles and 2 means that the number of particles has doubled when filtered with the new filter; factors less than 1 are not possible.

## Effect of engine parameters

### Part load results

Figure 2 shows the PN increase factor as the fuel injection timing is varied at test condition 2. Here, a PN increase factor of ~1.3 is observed for both

Filters 1 ( $D_{90}$  cut at 23 nm) and 2 ( $D_{90}$  cut at 15 nm), which is in line with previously reported results in the literature from GDI engines. With both filters, a  $\sim 0.1$  increase in PN increase factor is observed at the 320°btdc timing. This condition also showed the lowest overall particulate emissions, previously attributed to a reduction in fuel impingement on the piston. This may indicate that combustion of a more homogeneous fuel-air mixture leads to a larger number of particles below 23 nm. At this test condition, the mean particle size is large ( $\sim 100$  nm) and so this accounts for the minor difference in PN increase factor ( $\sim 0.05$ ) observed between Filter 1 and Filter 2.

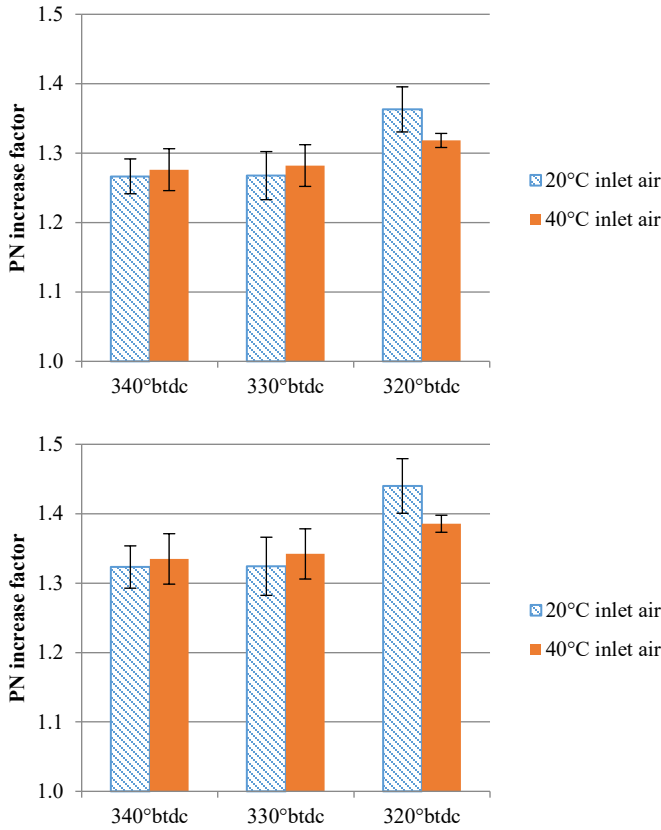


Figure 2: PN increase factor with Filter 1 (upper) and Filter 2 (lower) at 1250 rpm / 3.77 bar BMEP as inlet air temperature is increased from 20-40°C; the error bars correspond to  $\pm\sigma$ .

Figure 3 shows the PN increase factor as the spark timing is varied at test condition 2. Again all of the PN increase factors observed are  $\sim 1.3$  in line with results reported in the literature. While there is a minor increase observed as the spark timing is retarded, with both filters, there is no statistically significant result.

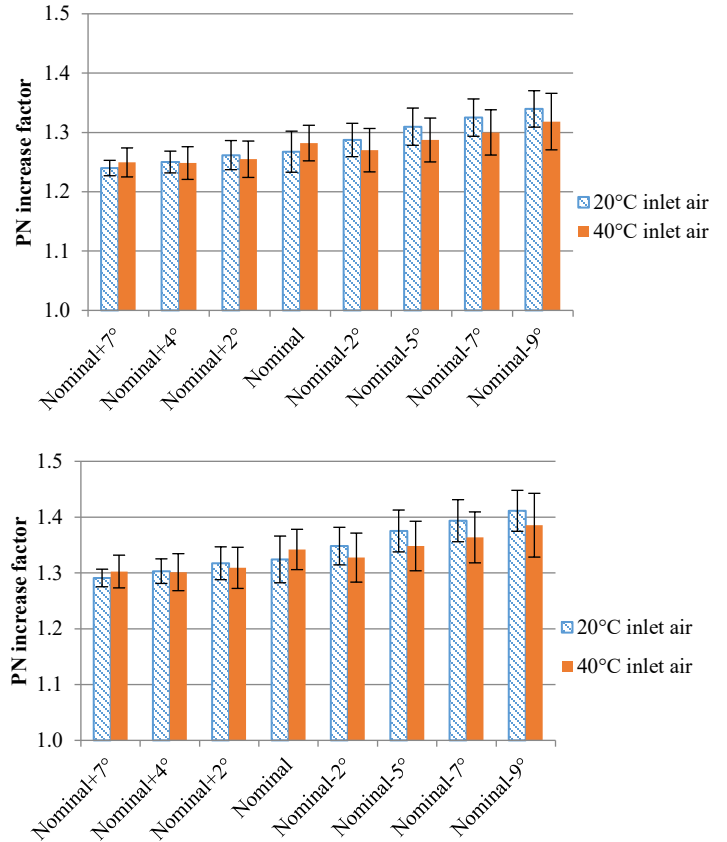


Figure 3: PN increase factor with Filter 1 (upper) and Filter 2 (lower) at 1250 rpm / 3.77 bar BMEP as inlet air temperature is increased from 20-40°C; the error bars correspond to  $\pm\sigma$ .

### Effect of inlet air temperature on PN emissions

In general, increasing the inlet air temperature will reduce PN emissions from GDI engines, as fuel evaporation is promoted [3]. Figure 2 and Figure 3 show that at part load, where inlet air temperature was varied from 20°C to 40°C, this parameter has no statistically significant effect on the PN increase factor with either filter.

### Effect of engine load on PN emissions

Figure 4 shows the PN increase factor as the engine load was increased at a fixed speed (2000 rpm). The UB100 engine operates with naturally aspirated breathing at lower loads, and boosted at higher loads. As the engine enters the boosted region (here, between 11 and 15 bar BMEP), there is a substantial change in engine calibration (cam lift and timing, injection timing, injection pressure, and spark timing to name a few significant parameters), and so the results between the two regions should not be compared directly. In Figure 4 it can be seen that in the naturally aspirated region, the PN increase factors are very low with both filters, and decrease as the load is increased. In the boosted region the PN increase factor is much higher – varying between  $\sim 1.4$  and  $\sim 1.6$ . Although the standard deviations are quite wide, it is clear that there is a peak in PN increase factor in the middle of the boosted range.

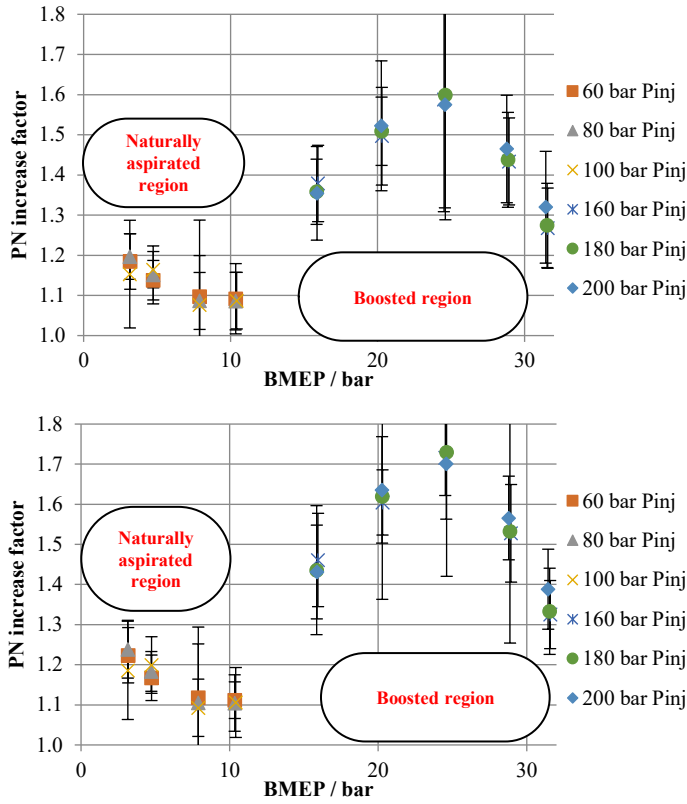


Figure 4: PN increase factor with Filter 1 (upper) and Filter 2 (lower) as engine load is increased from ~3 bar BMEP to ~32 bar BMEP at a speed of 2000 rpm with a stoichiometric mixture; the error bars correspond to  $\pm\sigma$

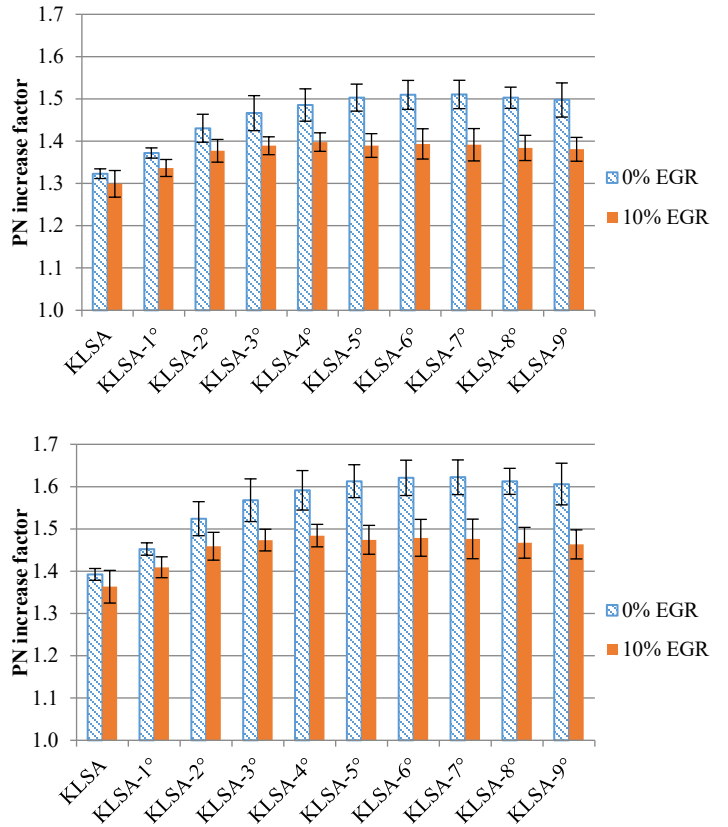


Figure 5: PN increase factor with Filter 1 (upper) and Filter 2 (lower) at 2000 rpm / full load as EGR is increased from 0-10%; the error bars correspond to  $\pm\sigma$ .

### Effect of fuel rail pressure on PN emissions

Fuel rail pressure typically has a substantial effect on PN emissions from GDI engines, with an increase in rail pressure leading to fewer PN emissions [3]. However, as can be seen in Figure 4, the effect of fuel rail pressure on the sub-23 nm particulates is not significant in these tests, with no significant differences being observed at any engine load.

### Full load results

Figure 5 shows the PN increase factor with the two filters as the EGR is increased from 0-10% at test condition 1 (2000 rpm / full load). At this test condition, high PN increase factors of 1.5 (Filter 1) and 1.6 (Filter 2) are observed, which are at the upper end of those reported in the literature. Adding cooled, external (low pressure), EGR increased the PN emissions from this engine, however it was also noted that the mean particle diameter increased with EGR from ~40 nm to ~50 nm. This is reflected in the PN increase factor when the particles below 23 nm are included. In Figure 5 it can be seen that at KLSA there is little difference in the PN increase factor with EGR, but as the spark is retarded (only by 2°), a lower PN increase factor (by approximately 0.1) is observed with the 10% EGR case. For both cases (0 & 10% EGR), when the spark is retarded at this condition there is a substantial rise in PN increase factor, by ~0.2 – perhaps suggesting that a rise in post-flame oxidation (expected with retarding the spark) is leading to a rise in sub-23 nm particles. In general Filter 2 leads to approximately a 0.1 increase in the PN increase factor.

Figure 6 shows the PN increase factor at test point 3 (3000 rpm, full load) as the EBP is increased from 1.7 barA to 2.2 barA, mimicking the transition from supercharged to turbocharged operation. Again, at this test point, retarding the spark from KLSA is leading to a rise in PN increase factor, although the rise is not as substantial as that observed at 2000 rpm / full load it is still notable. This rise is particularly noticeable with Filter 2 – indicating that there are substantial numbers of the smallest diameter particles present. There is no significant difference observed between Filter 1 and Filter 2, other than Filter 2 leading to a higher PN increase factor – as would be expected.

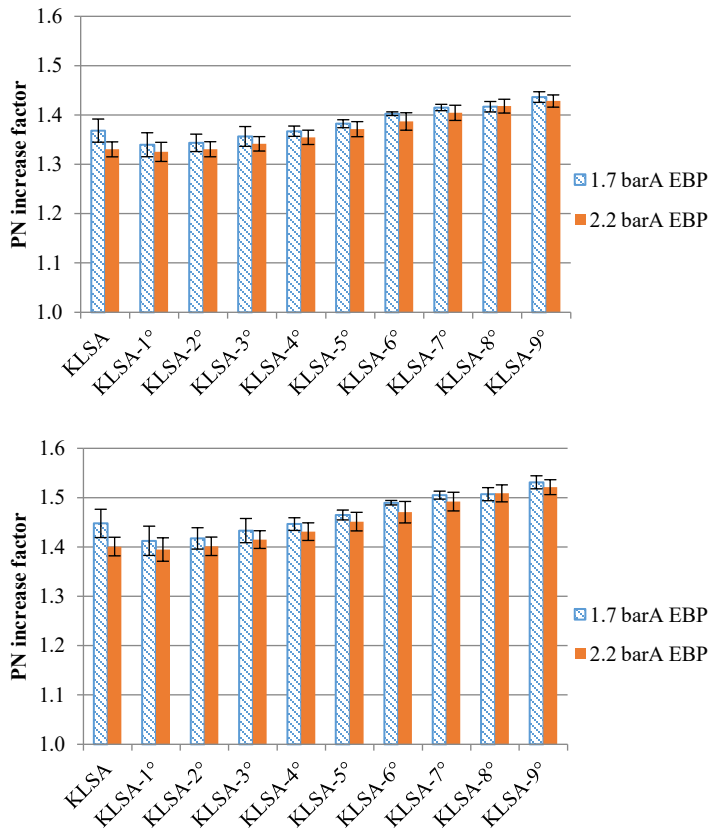


Figure 6: PN increase factor with Filter 1 (upper) and Filter 2 (lower) at 3000 rpm / full load as EBP is increased from 1.7-2.2 barA; the error bars correspond to  $\pm\sigma$ .

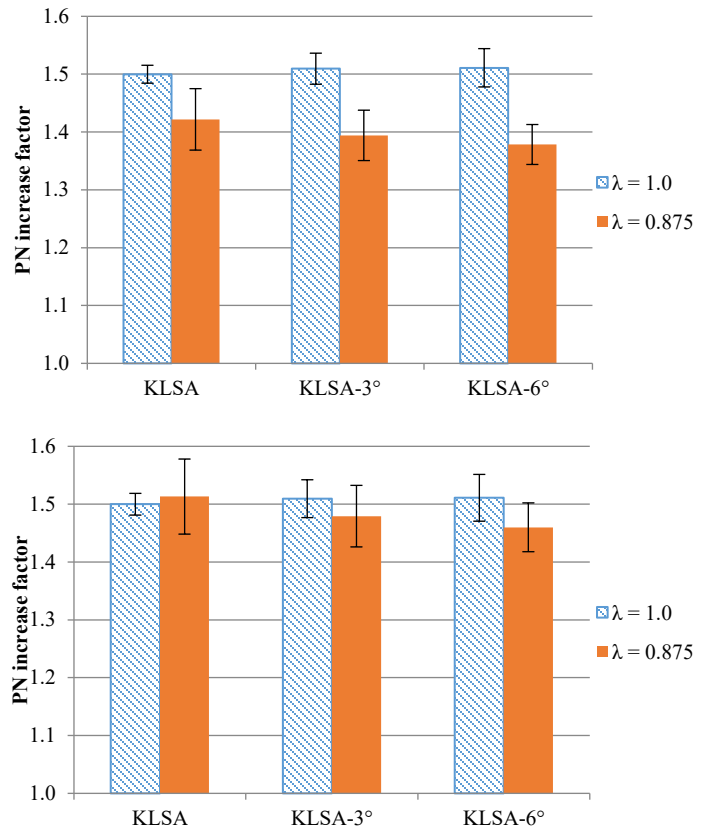


Figure 7: PN increase factor with Filter 1 (upper) and Filter 2 (lower) at 4000 rpm / full load as  $\lambda$  is decreased from 1.0-0.875; the error bars correspond to  $\pm\sigma$ .

Figure 7 shows the PN increase factor at test point 4 (4000 rpm, full load) as  $\lambda$  is decreased from 1.0 to 0.875. PN increase factors of  $\sim 1.5$  are again observed at this point. An increase in total PN as  $\lambda$  was decreased from 1.0 to 0.875 of around double-triple was observed in the previously reported results, as would be expected. Regarding the sub-23 nm particulates, the results show no significant difference between the two lambda cases with Filter 2, but a significant difference with Filter 1 with fewer particles sub-23 nm observed with Filter 1, suggesting that the particles that are included in Filter 2 are around 20 nm in diameter, which is where the main difference between the filters exists (see Figure 1).

## Effect of fuel composition

### Market representative fuels

#### Part load

Figure 8 shows the PN increase factor for market representative fuels at 1250 rpm / 3.77 bar BMEP. At this part load point, both Fuel H and I give very similar PN increase factors to the base fuel, with a slight decrease noted for Fuel I (the fuel representative of a market “premium” gasoline). The PN increase factor of these fuels continues to be insensitive to the inlet air temperatures tested, as before.

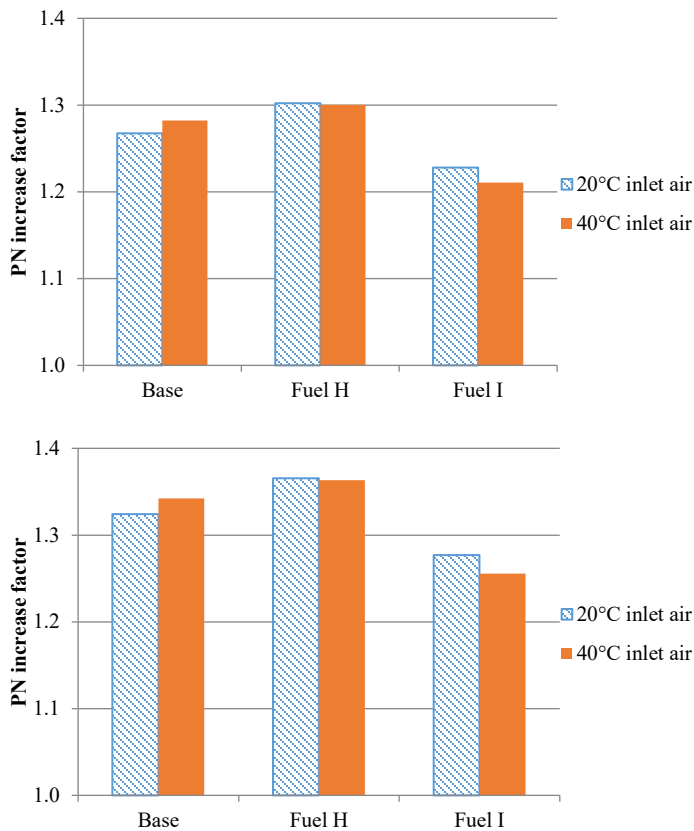


Figure 8: PN increase factor with Filter 1 (upper) and Filter 2 (lower) for market representative fuels at 1250 rpm / 3.77 bar BMEP as inlet air temperature is increased from 20-40°C.

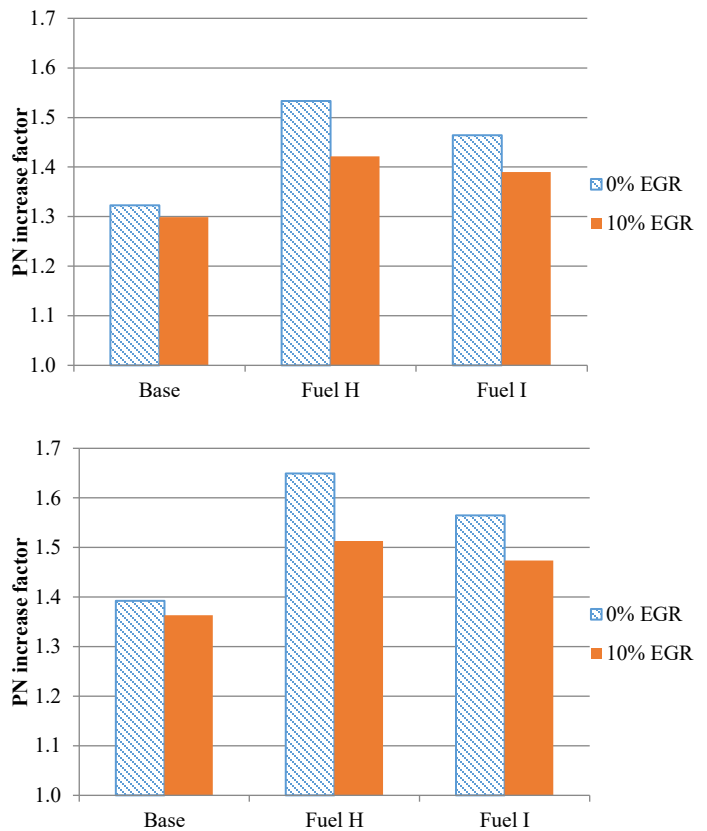


Figure 9: PN increase factor with Filter 1 (upper) and Filter 2 (lower) for market representative fuels at 2000 rpm / full load as EGR is increased from 0-10%.

### Full load

Figure 9 shows the PN increase factor for the market representative fuels at 2000 rpm / full load. Here, both Fuel H and I show a ~0.1 rise in PN increase factor compared to the base fuel. In addition, the trends observed previously of a minor decrease in PN increase factor with EGR holds here as well.

Figure 10 and Figure 11 show the PN increase factor for the market representative fuels at 3000 rpm / full load and 4000 rpm / full load respectively. Again, the trends seen at the other full load point with these fuels are observed, that Fuel H and I give a minor (~0.1-0.2) increase in sub-23 nm particulate emissions relative to the base fuel. The previously observed reduction in PN increase factor with increasing EBP and decreasing lambda are also noted here.

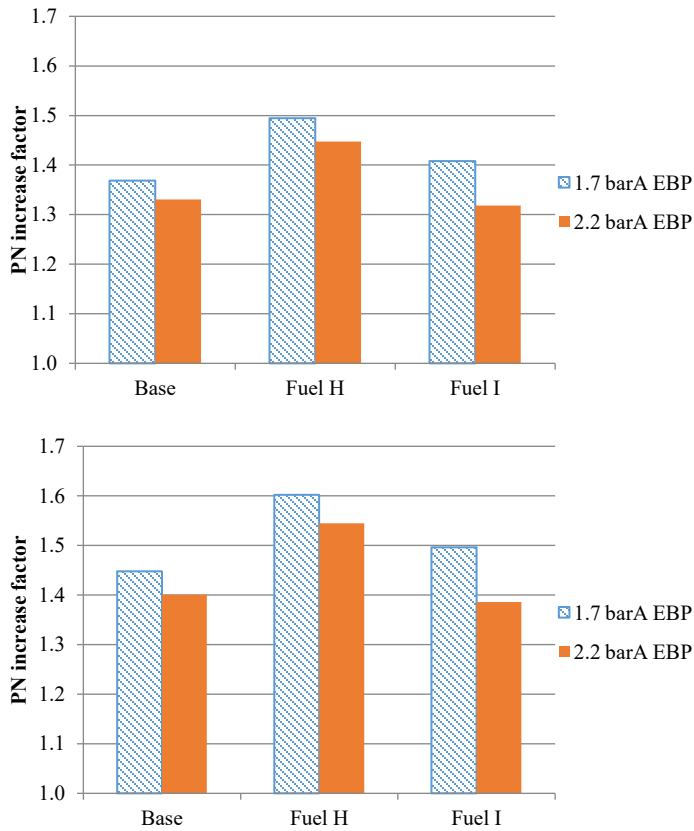


Figure 10: PN increase factor with Filter 1 (upper) and Filter 2 (lower) for market representative fuels at test condition 3 at 3000 rpm / full load as EBP is increased from 1.7-2.2 barA.

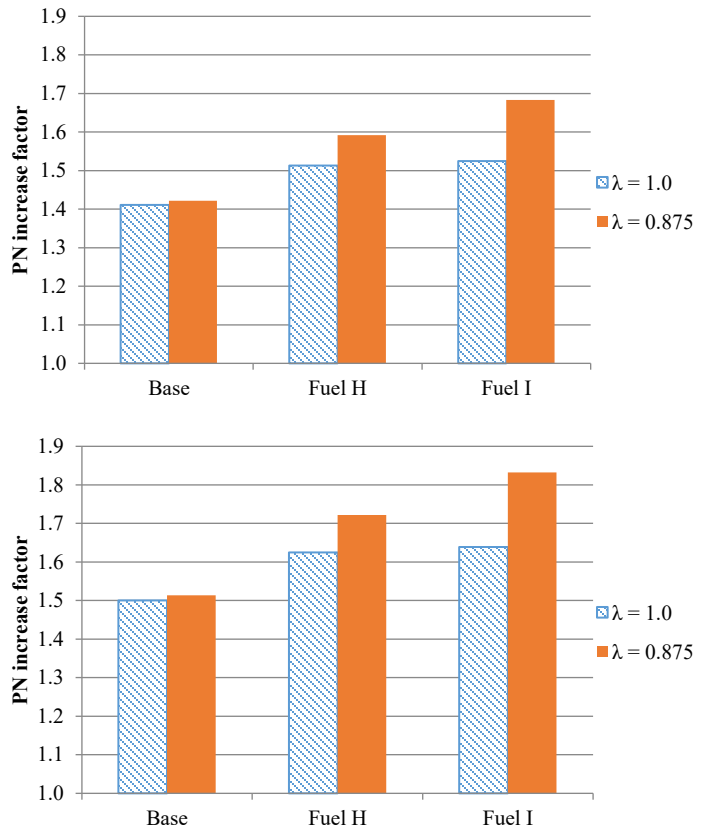


Figure 11: PN increase factor with Filter 1 (upper) and Filter 2 (lower) for market representative fuels at 4000 rpm / full load as  $\lambda$  is decreased from 1.0-0.875.

## Specially blended test fuels

### Part load

Figure 12 shows the PN increase factor for the specially blended test fuels at 1250 rpm / 3.77 bar BMEP. The first thing which is immediately observed is the very high PN increase factor ( $\sim 4$ ) for Fuel G. As discussed in [23] there is some evidence to suggest that the particles being emitted by Fuel G are volatile (in contrast to the other fuels), such as higher Unburned HydroCarbon (UHC) emissions which were observed at this test point (Figure 13). Such particles would not be counted by the PMP protocol or any of the other sub-23 nm particulate measurement projects in development at the moment – this is a clear limitation of the technique used in this work, but with the UHC results, an exception as obvious as this is clearly noted. Fuels A, C, and D emitted very low numbers of particles here, so the PN increase factors are subject to poor Signal-Noise Ratio (SNR). The PN increase factors seen with Fuels B, E, and F, are in agreement with those seen with all other fuels at this test point.



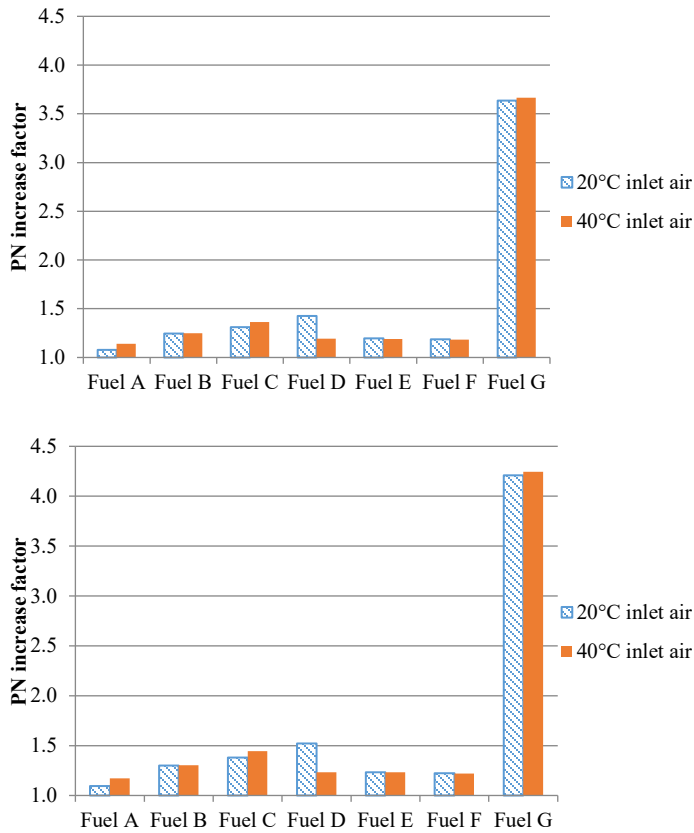


Figure 12: PN increase factor with Filter 1 (upper) and Filter 2 (lower) for specially blended test fuels at 1250 rpm / 3.77 bar BMEP as inlet air temperature is increased from 20-40°C.

PN increase factors ~0.1 higher compared to Filter 1, indicating that there are a significant proportion of particles between 10 and 23 nm, as this is where there is the largest difference in filter response.

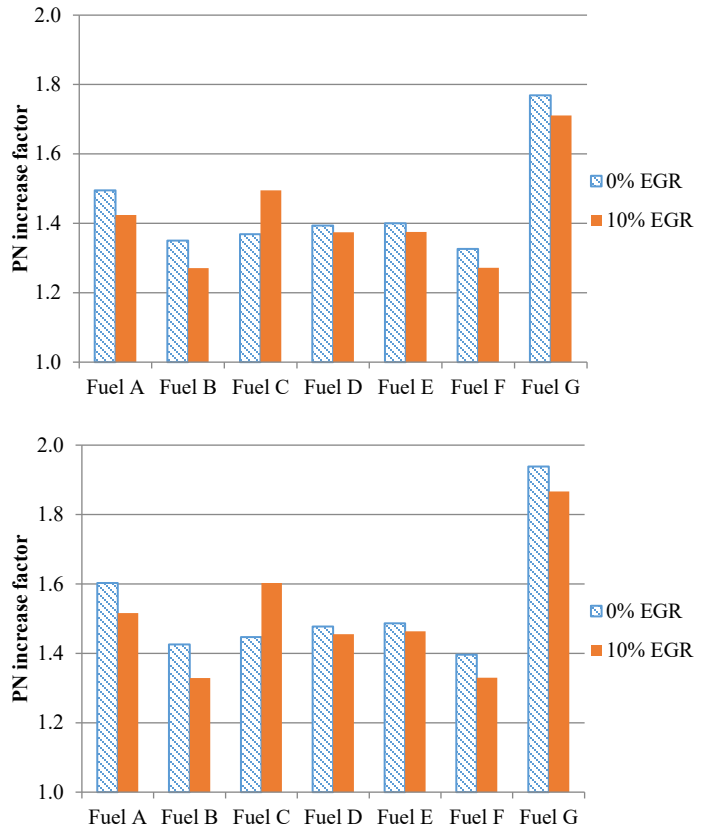


Figure 14: PN increase factor with Filter 1 (upper) and Filter 2 (lower) for specially blended test fuels at 2000 rpm / full load as EGR is increased from 0-10%.

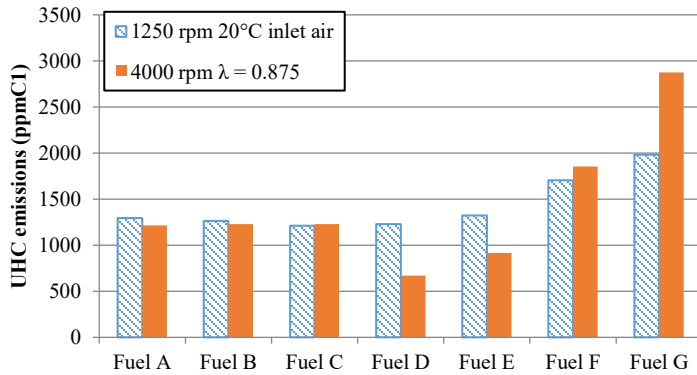


Figure 13: UHC emissions at 1250 rpm / 3.77 bar BMEP (inlet air temperature 20°C) and 4000 rpm / full load ( $\lambda = 0.875$ ).

### Full load

Figure 14 and Figure 15 shows the PN increase factor for the specially blended test fuels at 2000 rpm / full load and 3000 rpm / full load respectively. The results at these test points are similar to those observed for the market fuels at these test points. It is of note that Filter 2 leads to

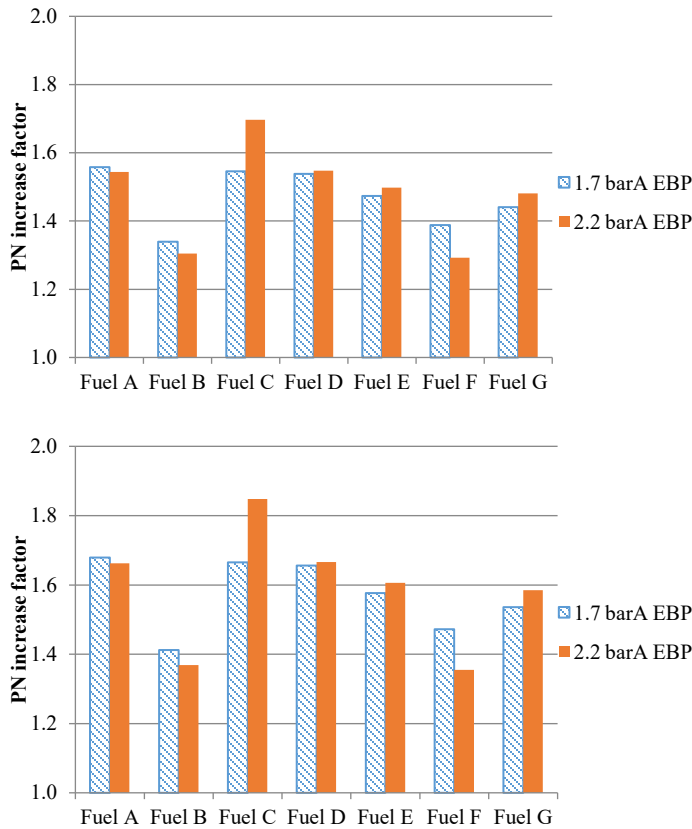


Figure 15: PN increase factor with Filter 1 (upper) and Filter 2 (lower) for specially blended test fuels at 3000 rpm / full load as EBP is increased from 1.7-2.2 barA.

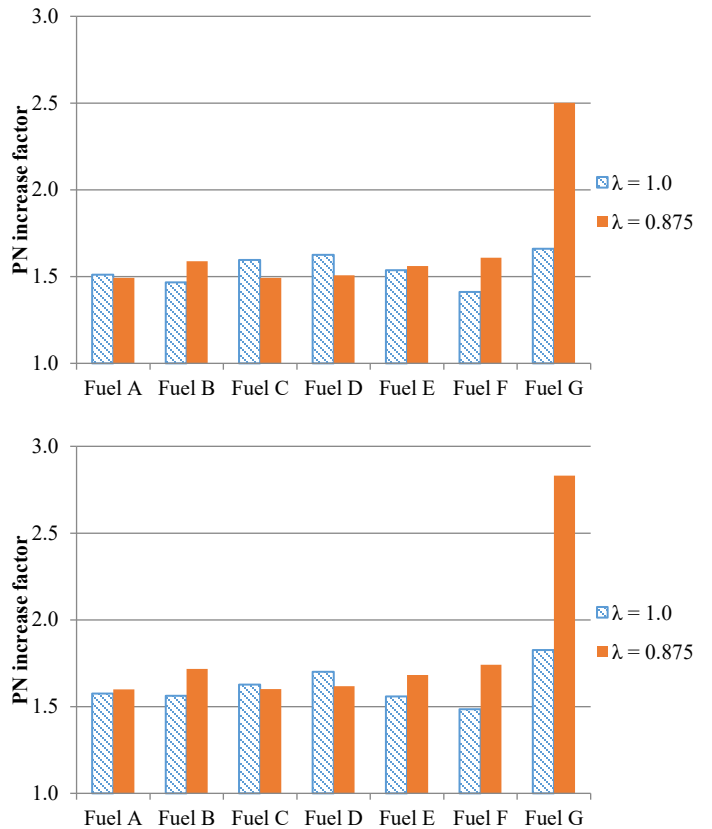


Figure 16: PN increase factor with Filter 1 (upper) and Filter 2 (lower) for specially blended test fuels at 4000 rpm / full load as  $\lambda$  is decreased from 1.0-0.875.

Figure 16 shows the PN increase factor for the specially blended test fuels at 4000 rpm / full load. Particularly at the  $\lambda = 0.875$  condition, the previously observed volatile particles from Fuel G are again responsible for the large PN increase factor for this fuel. The other PN increase factors here are in line with those for the other fuels at this test point (~1.6).

## Oxygenate fuels

### Part load

Figure 17 shows the PN increase factor for the oxygenate fuels at 1250 rpm / 3.77 bar BMEP. E20 can be seen to behave very similarly to the base fuel (see Figure 3) with PN increase factors ~1.3 observed. E85 shows much smaller PN increase factors, the smallest of any of the fuels tested – this fuel also emitted the lowest overall PN at this test condition. The GEM fuel has the lowest PN increase factor at 20°C inlet air temperature, and the highest (although still only ~1.3 – in line with the base fuel) at 40°C inlet air temperature. It is not known why such a minor variation in inlet air temperature is leading to such a major change in PN increase factor, however the overall PN emissions from this fuel were very low at this test point.

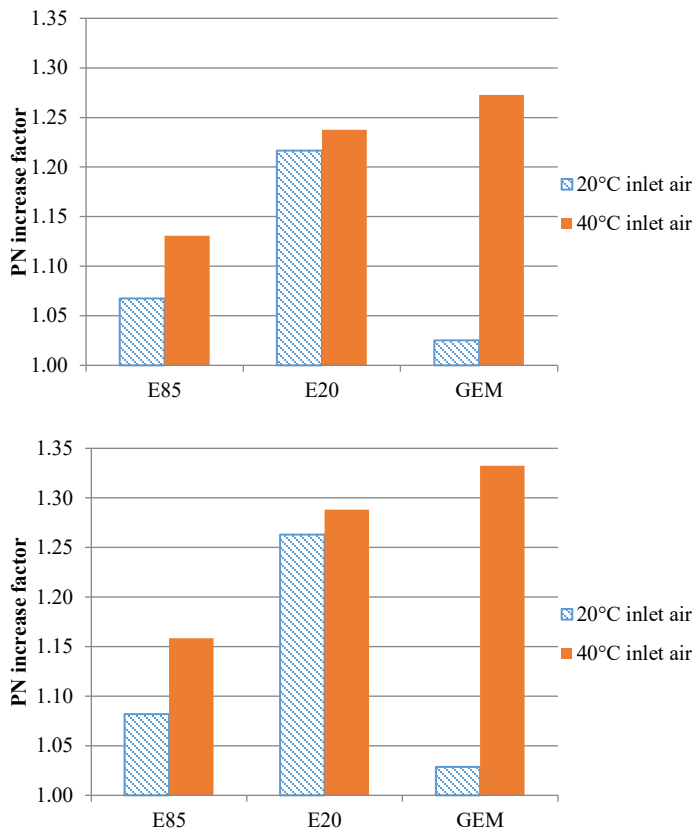


Figure 17: PN increase factor with Filter 1 (upper) and Filter 2 (lower) for oxygenate fuels at 1250 rpm / 3.77 bar BMEP as inlet air temperature is increased from 20-40°C.

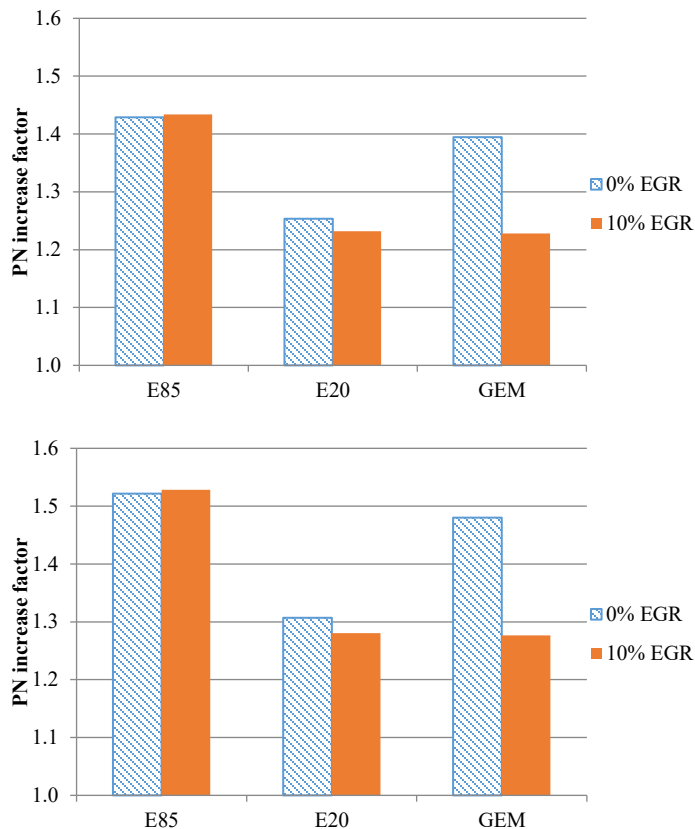


Figure 18: PN increase factor with Filter 1 (upper) and Filter 2 (lower) for oxygenate fuels at 2000 rpm / full load as EGR is increased from 0-10%.

### Full load

Figure 18 shows the PN increase factor for the oxygenate fuels at 2000 rpm / full load. The results for E85 and GEM (0% EGR) are similar to that from the baseline fuel (Figure 5). E20 and GEM (10% EGR) show a notable reduction in PN increase factor – in both cases, the reduction in PN increase factor can be attributed more to an increase in overall particles larger than 23 nm – rather than a decrease in sub-23 nm particles.

Figure 19 shows the PN increase factor for the oxygenate fuels at 3000 rpm / full load. E20 and GEM show very similar PN increase factors to the baseline fuel (Figure 6) and E85 shows a substantial rise in PN increase factor. The E85 fuel, however, emitted very low levels of particles (an order of magnitude lower than GEM), and so the total number of sub-23 nm particles may be proportionally higher, but is still very low overall – much lower than any of the other fuels.

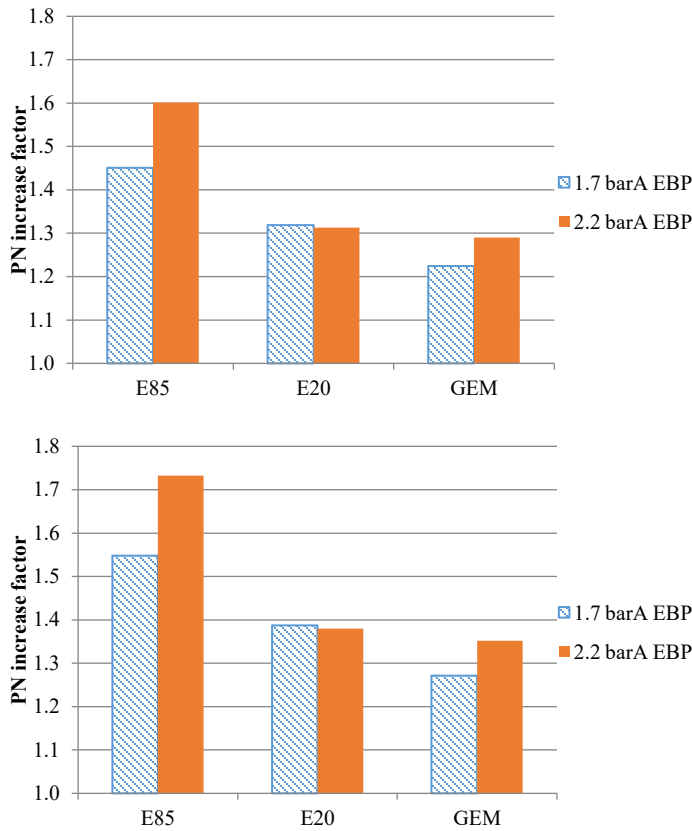


Figure 19: PN increase factor with Filter 1 (upper) and Filter 2 (lower) for oxygenate fuels at 3000 rpm / full load as EBP is increased from 1.7-2.2 barA.

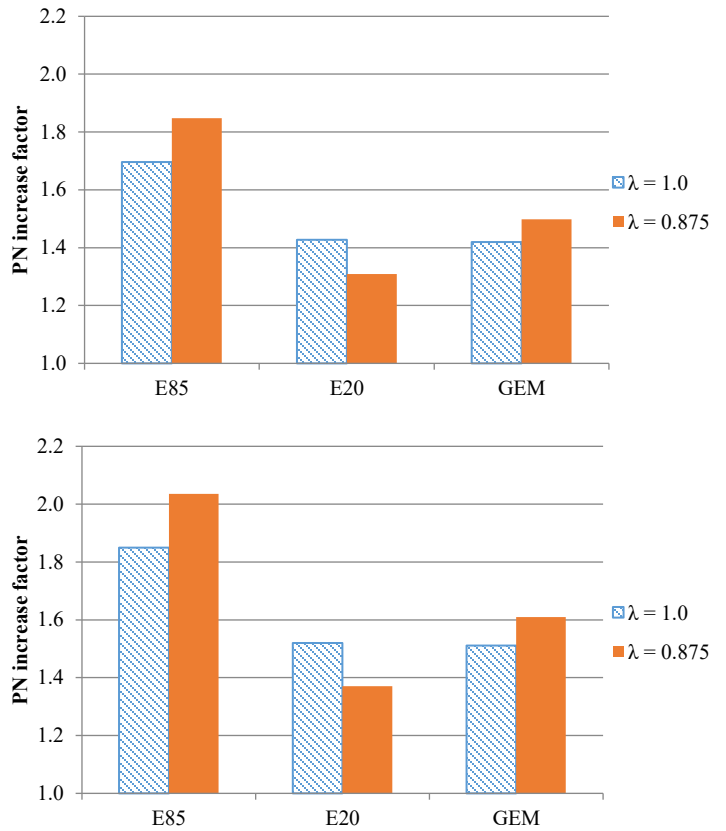


Figure 20: PN increase factor with Filter 1 (upper) and Filter 2 (lower) for oxygenate fuels at 4000 rpm / full load as  $\lambda$  is decreased from 1.0-0.875.

Figure 20 shows the PN increase factor for the oxygenate fuels at 4000 rpm / full load. The results are very similar to those at 3000 rpm / full load with a high PN increase factor for E85, which emitted the lowest levels of overall particles, and PN increase factors of ~1.3 for the other fuels – in line with the literature results for PN emissions from GDI engines.

## Discussion

### General observations

At part load, PN increase factors of 1.2-1.3 are observed – in line with literature data, suggesting that when  $D_{50}$  is moved from 23 nm to 10 nm, a 20-30% increase in PN emissions is observed from GDI engines. Advancing fuel injection timing led to an increase in the proportion of sub-23 nm particles emitted, whereas spark timing and inlet air temperature did not appear to have a significant effect. Increasing the load led to minor decreases in the proportion of sub-23 nm particles emitted, and the results were insensitive to fuel pressure.

At full load, overall higher levels of sub-23 nm particles were observed – with the proportion of sub-23 nm particles emitted being 40-60% at the upper end of those reported in the literature (but still within range). This is to be expected given the ~30 nm accumulation mode diameters previously reported for this dataset [17, 22, 23]. It is interesting that operating this engine at full load and highly boosted is the operating region where these highest levels are observed (as opposed to the 20-30% increase in sub-23 nm particles seen at part load) – this may explain the variation seen in the literature. Retarding the spark led to a notable (20%) increase in the proportion of sub-23 nm particles emitted at all three engine speeds tested. Increasing EGR from 0-10% led to a decrease in the proportion of sub-23 nm particles emitted, however EBP and lambda did not lead to significant differences.

## Comparison between Filter 1 and Filter 2

With the baseline fuel, Filter 2 ( $D_{90}$  cut at 15 nm) led to a roughly 8 percentage point increase in the proportion of sub-23 nm particles observed compared to Filter 1 ( $D_{90}$  cut at 23 nm) across all engine operating points. Filter 1 giving a 36% increase on average and Filter 2 a 45% increase on average. Across all fuels (excluding Fuel G) and operating points Filter 1 gives a 38% increase on average and Filter 2 a 47% increase on average. The biggest difference between these two filters occurs between 10 and 23 nm (see Figure 1), and so the sub-23 nm PN emissions from this engine appear to be concentrated in this area. Given the shapes of the two filters and the specifications of the CPCs under consideration by the projects to replace the current PMP procedure, it is likely that Filter 2 will be a better predictor of the sub-23 nm PN emissions.

## Fuel composition

Inevitably different fuels led to different PN increase factors, and it is difficult to draw general conclusions. However, in general no one type of fuel led to significant differences in the proportion of sub-23 nm particles emitted. E20 and GEM had very low proportions of sub-23 nm particles at full load, in contrast with most of the other fuels tested. In contrast, E85 had very high levels of sub-23 nm particles but in the context of very low overall emissions [22]. Fuel G, had a very large number of sub-23 nm particles, however there is evidence to suggest that those particles are volatile which would not be counted by the PMP protocol and typically removed by a three-way catalyst (TWC) in a production vehicle.

## Summary / Conclusions

The proportion of particles less than 23 nm in diameter emitted from a prototype highly boosted engine, varying a number of engine parameters and with fourteen different fuels, has been evaluated in accordance with two proposed methods for counting such particles. These PN emissions have been measured with a DMS500, and evaluated with two Wiebe filtering methodologies, which are derived from a previous Wiebe filter shown to represent the PMP protocol closely.

In general Filter 2 counted nine percentage points more particles than Filter 1. Given the shapes of the filters, and the CPCs under consideration by groups proposing sub-23 nm particle measurement updates to the PMP, Filter 2 is likely to be more representative. However further work to validate the digital filtering approach against whatever new PMP protocols may be adopted will be needed. In particular, the approach proposed in this work does not guarantee that no volatile particles, which are removed under PMP and by TWCs fitted to production engines, will be counted. That said, when combined with other measurements (such as the UHC emissions) – significant outliers in this respect can be discounted.

At part load, PN increase factors in line with those reported in the literature (~1.3) are observed, this gives confidence in the methodology used to obtain these results. At high BMEPs, high PN increase factors (~1.5 and above) are observed, this means that were the PMP  $D_{50}$  moved to 10 nm, a ~50% increase in particulates might be expected to be observed from highly boosted GDI engines at full load. This observation is in line with other evidence presented in the literature.

## References

1. Andersson, J., et al., *Particle Measurement Programme (PMP) Light-duty Inter-laboratory Correlation Exercise (ILCE\_LD) Final Report*. 2007, European Commission Joint Research Centre Institute for Environment and Sustainability.
2. Eastwood, P., *Particulate Emissions from Vehicles*. 2008: SAE International and John Wiley & Sons, Ltd. ISBN: 978-0-470-98650-9.
3. Raza, M., et al., *A Review of Particulate Number (PN) Emissions from Gasoline Direct Injection (GDI) Engines and Their Control Techniques*. *Energies* **11**(6):1417, 2018. <https://doi.org/10.3390/en11061417>
4. Zhao, H., *Overview of Gasoline Direct Injection Engines*, in *Advanced direct injection combustion engine technologies and development: Gasoline and gas engines*. 2010, Woodhead Publishing Ltd. ISBN: 978-1-845-69389-3.
5. Martini, G., B. Giechaskiel, and P. Dilara, *Future European emission standards for vehicles: the importance of the UN-ECE Particle Measurement Programme*. *Biomarkers* **14**(sup1):29-33, 2009. <https://doi.org/10.1080/13547500902965393>
6. Gidney, J.T., M.V. Twigg, and D.B. Kittelson, *Effect of Organometallic Fuel Additives on Nanoparticle Emissions from a Gasoline Passenger Car*. *Environmental Science & Technology* **44**(7):2562-2569, 2010. <https://doi.org/10.1021/es901868c>
7. Giechaskiel, B., Manfredi, U., and Martini, G., *Engine Exhaust Solid Sub-23 nm Particles: I. Literature Survey*, *SAE Int. J. Fuels Lubr.* **7**(3):950-964, 2014, <https://doi.org/10.4271/2014-01-2834>
8. Jang, J., et al., *Reduction of particle emissions from gasoline vehicles with direct fuel injection systems using a gasoline particulate filter*. *Science of The Total Environment* **644**:1418-1428, 2018. <https://doi.org/10.1016/j.scitotenv.2018.06.362>
9. Zheng, Z., et al., *Investigation of solid particle number measurement: Existence and nature of sub-23nm particles under PMP methodology*. *Journal of Aerosol Science* **42**(12):883-897, 2011. <https://doi.org/10.1016/j.jaerosci.2011.08.003>
10. *Procedure for the Continuous Sampling and Measurement of Non-Volatile Particulate Matter Emissions from Aircraft Turbine Engines*. SAE Standard: ARP6320, 2018, SAE International.
11. Giechaskiel, B., et al., *Investigation of vehicle exhaust sub-23 nm particle emissions*. *Aerosol Science and Technology* **51**(5):626-641, 2017. <https://doi.org/10.1080/02786826.2017.1286291>
12. *Down To Ten*. Available from: <http://www.downtoten.com/>. (accessed 7 March 2019)
13. *SUREAL-23*. Available from: <http://sureal-23.cperi.certh.gr>. (accessed 7 March 2019)
14. *PEMs4Nano*. Available from: <http://www.pems4nano.eu>. (accessed 7 March 2019)
15. Giechaskiel, B., et al., *Particle number measurements in the European legislation and future JRC activities*. *Combustion Engines* **74**(3):3-16, 2018. <https://doi.org/10.19206/CE-2018-301>
16. Johansson, A. and Dahlander, P., *Experimental Investigation of the Influence of Boost on Combustion and Particulate Emissions in Optical and Metal SGDI-Engines Operated in Stratified Mode*, *SAE Int. J. Engines* **9**(2):807-818, 2016. <https://doi.org/10.4271/2016-01-0714>
17. Leach, F., et al., *Particulate emissions from a highly boosted Gasoline Direct Injection engine*. *International Journal of*

- Engine Research **19**(3):347–359, 2018.  
<https://doi.org/10.1177/1468087417710583>
18. Karjalainen, P., et al., *Exhaust particles of modern gasoline vehicles: A laboratory and an on-road study*. Atmospheric Environment **97**:262-270, 2014.  
<https://doi.org/10.1016/j.atmosenv.2014.08.025>
  19. Bogarra, M., et al., *Influence of Three-Way Catalyst on Gaseous and Particulate Matter Emissions During Gasoline Direct Injection Engine Cold-start*. Johnson Matthey Technology Review **61**(4):329-341, 2017.  
<https://doi.org/10.1595/205651317X696315>
  20. Braisher, M., Stone, R., and Price, P., *Particle Number Emissions from a Range of European Vehicles*, SAE Technical Paper 2010-01-0786, 2010. <https://doi.org/10.4271/2010-01-0786>
  21. Leach, F., et al., *Predicting the particulate matter emissions from spray-guided gasoline direct-injection spark ignition engines*. Proceedings of the Institution of Mechanical Engineers, Part D: Journal of Automobile Engineering **231**(6):717-730, 2017. <https://doi.org/10.1177/0954407016657453>
  22. Leach, F.C.P., et al., *The effect of oxygenate fuels on PN emissions from a highly boosted GDI engine*. Fuel **225**:277-286, 2018. <https://doi.org/10.1016/j.fuel.2018.03.148>
  23. Leach, F.C.P., et al., *The effect of fuel composition on particulate emissions from a highly boosted GDI engine – an evaluation of three particulate indices*. Fuel. **252**:598-611, 2019. <https://doi.org/10.1016/j.fuel.2019.04.115>
  24. Reavell, K., Hands, T., and Collings, N., *A Fast Response Particulate Spectrometer for Combustion Aerosols*, SAE Technical Paper 2002-01-2714, 2002.  
<https://doi.org/10.4271/2002-01-2714>
  25. Horn, H., *Calibrated CPC with D50 ≤ 10 nm for laboratory use – together with the documented calibration procedure*. PEMs4Nano deliverable D2.2, 2017. Available from: [http://www.pems4nano.eu/download/public\\_reports/reports\\_of\\_project\\_results\\_deliverables/PEMs4Nano\\_D2.2\\_Calibrated\\_CP\\_C\\_for\\_lab\\_use\\_with\\_calibration\\_procedure\\_PU.pdf](http://www.pems4nano.eu/download/public_reports/reports_of_project_results_deliverables/PEMs4Nano_D2.2_Calibrated_CP_C_for_lab_use_with_calibration_procedure_PU.pdf)
  26. Turner, J., Popplewell, A., Patel, R., Johnson, T. et al., *Ultra Boost for Economy: Extending the Limits of Extreme Engine Downsizing*, SAE Int. J. Engines **7**(1):387-417, 2014.  
<https://doi.org/10.4271/2014-01-1185>
  27. Leach, F., Knorsch, T., Laidig, C., and Wiese, W., *A Review of the Requirements for Injection Systems and the Effects of Fuel Quality on Particulate Emissions from GDI Engines*, SAE Technical Paper 2018-01-1710, 2018,  
<https://doi.org/10.4271/2018-01-1710>
  28. Leach, F., Stone, R., and Richardson, D., *The Influence of Fuel Properties on Particulate Number Emissions from a Direct Injection Spark Ignition Engine*, SAE Technical Paper 2013-01-1558, 2013, <https://doi.org/10.4271/2013-01-1558>
  29. EN228:2008 Automotive fuels. Unleaded petrol. Requirements and test methods. 2008.

## Contact Information

Felix Leach,  
 Dept of Engineering Science  
 University of Oxford  
 Parks Rd  
 Oxford

OX1 3PJ  
 UK

[felix.leach@eng.ox.ac.uk](mailto:felix.leach@eng.ox.ac.uk)

## Acknowledgments

The authors acknowledge the Technology Strategy Board (now Innovate UK), the UK's innovation agency, for the partial funding of this work. Consortium members GE Precision Engineering, Lotus Engineering, CD-Adapco, Imperial College London, University of Bath and the University of Leeds have all made various portions of this work possible.

This work was funded by Jaguar Land Rover, Shell, and the Technology Strategy Board (now Innovate UK). In addition, all of the project partners listed above made contributions.

## Definitions/Abbreviations

<b>DMS</b>	Differential Mobility Spectrometer
<b>d<sub>p</sub></b>	Particle diameter
<b>EBP</b>	Exhaust Back Pressure
<b>EGR</b>	Exhaust Gas Recirculation
<b>EU</b>	European Union
<b>Filter 1</b>	Digital Wiebe filter with D <sub>90</sub> cut at 23 nm
<b>Filter 2</b>	Digital Wiebe filter with D <sub>90</sub> cut at 15 nm
<b>GDI</b>	Gasoline Direct Injection
<b>GEM</b>	Gasoline, Ethanol, and Methanol
<b>JRC</b>	Joint Research Centre
<b>KLSA</b>	Knock Limited Spark Advance
<b>PFI</b>	Port Fuel Injection
<b>PN</b>	Particle Number
<b>SNR</b>	Signal-Noise Ratio
<b>TWC</b>	Three Way Catalyst
<b>UHC</b>	Unburned HydroCarbon
<b>WOT</b>	Wide Open Throttle